HHS Public Access
Author manuscript
J Mol Cell Cardiol. Author manuscript; available in PMC 2023 March 01.

Published in final edited form as:
J Mol Cell Cardiol. 2022 March ; 164: 1–12. doi:10.1016/j.yjmcc.2021.11.002.

Bone marrow- or adipose-mesenchymal stromal cell secretome preserves myocardial transcriptome profile and ameliorates cardiac damage following ex vivo cold storage

Susan R Scott[1], **Keith L March**[3,5], **I-wen Wang**[1,2], **Kanhaiya Singh**[1,4], **Jianyun Liu**[1], **Mark Turrentine**[1], **Chandan K Sen**[1,4], **Meijing Wang**[1]

[1]Department of Surgery, IU School of Medicine, Indianapolis, IN, U.S.A

[2]Methodist Hospital, IU Health, IU School of Medicine, Indianapolis, IN, U.S.A

[3]Division of Cardiovascular Medicine, Department of Medicine, IU School of Medicine, Indianapolis, IN, U.S.A

[4]Indiana Center for Regenerative Medicine and Engineering, Indiana University School of Medicine, Indianapolis, Indiana, U.S.A

[5]Division of Cardiovascular Medicine, Center for Regenerative Medicine, University of Florida, Gainesville, FL, U.S.A

Abstract

Background: Heart transplantation, a life-saving approach for patients with end-stage heart disease, is limited by shortage of donor organs. While prolonged storage provides more organs, it increases the extent of ischemia. Therefore, we seek to understand molecular mechanisms underlying pathophysiological changes of donor hearts during prolonged storage. Additionally, considering mesenchymal stromal cell (MSC)-derived paracrine protection, we aim to test if MSC secretome preserves myocardial transcriptome profile and whether MSC secretome from a certain source provides the optimal protection in donor hearts during cold storage.

Methods and Results: Isolated mouse hearts were divided into: no cold storage (control), 6hr cold storage (6hr-I), 6hr-I+conditioned media from bone marrow MSCs (BM-MSC CM), and 6hr-I+adipose-MSC CM (Ad-MSC CM). Deep RNA sequencing analysis revealed that compared to control, 6hr-I led to 266 differentially expressed genes, many of which were implicated in modulating mitochondrial performance, oxidative stress response, myocardial function, and apoptosis. BM-MSC CM and Ad-MSC CM restored these gene expression towards control. They also improved 6hr-I-induced myocardial functional depression, reduced inflammatory cytokine production, decreased apoptosis, and reduced myocardial H_2O_2. However, neither

Correspondence: Meijing Wang, MD, 950 W. Walnut Street, R2 E319, Indianapolis, Indiana 46202, meiwang@iupui.edu, Phone: 317-274-0827.

Conflict of Interest: None.

MSC-exosomes nor exosome-depleted CM recapitulated MSC CM-ameliorated apoptosis and CM-improved mitochondrial preservation during cold ischemia. Knockdown of Per2 by specific siRNA abolished MSC CM-mediated these protective effects in cardiomyocytes following 6hr cold storage.

Conclusions: Our results demonstrated that using MSC secretome (BM-MSCs and Ad-MSCs) during prolonged cold storage confers preservation of the normal transcriptional "fingerprint", and reduces donor heart damage. MSC-released soluble factors and exosomes may synergistically act for donor heart protection.

Graphics Abstract

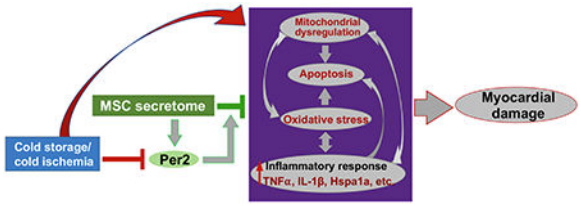

Introduction

Although therapies for heart disease have greatly improved over the past several decades, heart transplantation remains the ultimate treatment for the increased number of patients who develop terminal heart failure. Currently, there are > 250,000 people in the U.S.A. at the end-stages of heart failure and approximately 15% of them are in an urgent need for heart transplant. Based on OPTN/SRTR (Organ Procurement and Transplantation Network/ Scientific Registry of Transplant Recipients) 2018 Annual Data Report, new waiting lists for heart transplantation continued to increase, with 3883 new adult candidates in 2018 (resulting in > 7,400 candidates during the course of a year) [1]. However, only 2967 transplants occurred in adult recipients [1], largely due to a severe shortage of organ supply. Therefore, it is critical to increase the number of suitable donor hearts for transplantation.

One important reason for donor heart shortage is progressive quality deterioration after removal from donors, which is attributable to ischemic damage during *ex vivo* storage. As a result, there is a limited time window permitted between procurement of hearts and their implantation. In most medical centers, this time window is narrowed to 4-6 hours. Such limited transport/storage time by which hearts must be re-implanted to minimize ischemic injury is an important factor, rendering many potentially available donor hearts unusable. This particularly affects potential recipients in distant geographical areas. In fact, despite the lack of available organs, about 60% of obtainable donor hearts are not utilized for clinical transplantation largely because of deterioration during transit [2]. Therefore, utilizing effective strategies to modify preservation solution is appealing since it can prolong storage time, increase donor heart utilization, and improve graft function after transplantation.

Of note, mesenchymal stromal cell (MSC)-based therapy has emerged as promising approach for treatment of heart disease. Evidence from others and our group has shown MSC-derived paracrine protection on tissue/organs against ischemia [3–8]. However, the overwhelming majority of studies on using MSCs for cardiac preservation or repair have

been mainly focusing on ischemic heart disease and heart failure [9–13]. Little information exists regarding the potential of MSC-derived therapy in heart transplantation. MSCs can be obtained from many tissues, including bone marrow, adipose, umbilical cord, etc. A recent study has shown that by using hypothermic oxygenated perfusion to store donor hearts, bone marrow MSC (BM-MSC)-conditioned media (CM) added to perfusion solution improved myocardial function in grafts donated from 15-month-old rats [14]. More importantly, we are the first to indicate that supplementing BM-MSC secretome to preservation solution protected donor organ performance against cold static storage-induced ischemia and subsequent reperfusion injury using an *in vivo* murine heterotopic heart transplantation model [15]. We have also indicated that adipose-derived MSC (Ad-MSC) secretome improved contractile activity and viability in human-induced pluripotent stem cell-derived cardiomyocytes exposed to cold preservation solution (mimicking cold static storage of donor hearts) [16]. However, it is unclear whether MSCs derived from various tissue sources have different therapeutic efficacy on donor heart preservation during cold storage.

Furthermore, cold storage/ischemia may lead to dynamic changes of myocardial transcriptome expression profile. It is unknown whether adding MSC secretome to storage solution could preserve cold ischemia-induced alterations of myocardial transcriptome profile. Therefore, in this study, we aim to determine whether 6hr cold storage (6hr-I) induces myocardial transcriptome changes and the effect of BM-MSC and Ad-MSC secretome on maintaining myocardial transcriptome profile following *ex vivo* cold storage. We also seek to compare the therapeutic potential of BM-MSC secretome with Ad-MSC secretome (when added to preservation solution) on ameliorating cold ischemia and subsequent reperfusion (I/R)-damaged donor hearts, by evaluating myocardial function and inflammatory cytokine production, as well as the degree of cell death.

Methods and Materials

Animals

C57BL/6J mice (male, 10-15 weeks) were purchased from the Jackson Laboratories (Bar Harbor, ME) and acclimated with a standard diet feeding for > 1 week before the experiments. The animal protocol was reviewed and approved by the Institutional Animal Care and Use Committee of Indiana University. All animals received humane care in compliance with the *Guide for the Care and Use of Laboratory Animals (*NIH Pub. No. 85-23, revised 1996).

Preparation of CM from human BM-MSCs and Ad-MSCs

Human BM-MSCs (PT-2501) and Ad-MSCs (PT-5006) were purchased and characterized by the company (Lonza Walkersville Inc., Walkersville, MD). These cells were tested for purity of cell surface markers (positive for CD29, CD44, CD73, CD90, CD105, and CD166, but negative for CD14, CD34, and CD45), and for their ability to differentiate into osteogenic, chondrogenic, and adipogenic lineages. The cells were cultured with MSC growth medium or ADSC growth medium respectively, based on the manufacturer's instructions (Lonza) and our previous experience [4]. CM was generated as shown in Figure

S1. Briefly, the supernatant was sequentially concentrated to 100-fold by centrifugation through the Amicon Ultra Centrifugal Filter (membranes cutoff >3 kDa, EMD Millipore) as we previously described [15, 17]. The concentrated CM from the filtrate tube of the top unit was diluted in University of Wisconsin (UW) solution to the final concentration as indicated in Figure S1A. The BM-MSC CM and Ad-MSC CM were used in experimental groups as shown in Figure S2. We did not observe any difference in cell morphology and growth rate between BM-MSCs and Ad-MSCs during the culture (Figure S3).

Preparation of BM MSC-derived exosomes and BM MSC-CM^{GW4689}

Exosomes (Exo) were isolated from the concentrated BM-MSC CM using ExoQuick-TC exosome isolation kit (System Biosciences) (Figure S1B). Transmission electron microscope (TEM) was used to evaluate Exo morphology and Nanosight analysis was employed to determine size distribution of Exo.

GW4869 (an exosome release inhibitor, 10 μM) was utilized to treat BM-MSCs [15, 18]. After 72hr treatment, the BM-MSC CM was collected, centrifuged, and concentrated to obtain exosome-depleted MSC-CM (Figure S1C).

Next-generation RNA sequencing using Ion Proton Semiconductor standard methods

Total RNA was extracted using miRNeasy Mini kit (Qiagen) from mouse hearts of two experiments. One performed as baseline control (non-ischemia, n=4 hearts) vs. 6hr-I (n =3 hearts) and another set as baseline control (n = 3), 6hr-I + vehicle (n = 3), 6hr-I + BM-MSC CM (n = 4), and 6hr-I + Ad-MSC CM (n = 4). Total heart RNA was evaluated for quantity and quality using Agilent Bioanalyzer. 500 ng of total RNA was used. cDNA library preparation included polyA mRNA capture, enzymatic fragmentation, hybridization and ligation of adaptors, reverse transcription, size-selection, and amplification with barcode primers, following the Ion Total RNA-Seq Kit v2 User Guide (Life Technologies). Each resulting barcoded library was quantified and its quality accessed by Agilent Bioanalyzer and multiple libraries pooled in equal molarity. Eight μl of 100 pM pooled libraries were applied to Ion Sphere Particles (ISP) template preparation and amplification using Ion OneTouch 2, followed by ISP loading onto PI chip and sequencing on Ion Proton semiconductor. It was obtained for expression of 13,068 genes, with approximately 20 million reads per heart. The multi-dimensional scaling (MDS) plots were shown in Figure S4. Significantly differentially expressed genes were subjected to functional analysis using Ingenuity Pathway Analysis (IPA) as we previously described [19–21].

Real-time quantitative PCR

Total RNA was extracted from human left ventricle (LV) stored in cold preservation solution at 0-4°C using miRNeasy Mini kit (n = 3 hearts/group) and mouse hearts subjected to 6hr cold storage + vehicle, MSC-Exo, or MSC-CM^{GW4689}. The same amount of total RNA from each preparation was used for the first-strand cDNA reverse transcription using Quantum (ThermoFisher Scientific). Transcript levels were then determined by Real-time PCR (7500 Real-Time PCR System, Applied Biosystems) using TaqMan assays for Per2 (period circadian regulator 2), Arntl/Bmal1 (Aryl hydrocarbon receptor nuclear translocator-like protein 1 or Brain and Muscle ARNT-Like 1), and GAPDH or 18S rRNA (ThermoFisher

Scientific). The expression of Per2 and Arntl/Bmal1 was normalized to GAPDH or 18S rRNA levels using the standard $2^{-\Delta CT}$ methods.

Isolated mouse heart preparation (Langendorff)

Mouse hearts were isolated and immediately received coronary infusion of 1 ml of cold UW solution with vehicle, BM-MSC CM, or Ad-MSC CM, as previously described [15]. The hearts were then stored in a tube containing same solution on ice, emulating the conditions commonly used by medical centers during transport of hearts. After 6 hours, the hearts were transferred to a Langendorff prep and then perfused in the isovolumetric Langendorff mode (70 mmHg) for 60 minutes as mentioned in our previous studies [4, 17, 22–25]. Data of left ventricular (LV) function were recorded using a PowerLab 8 preamplifier/digitizer (AD Instruments Inc., Milford, MA). The maximal positive and negative values of the first derivative of pressure (+ dP/dt and −dP/dt) were calculated using PowerLab software. To better understand the workload of the heart, we also utilized rate pressure product (RPP = LV developed pressure x Heart rate). Mouse hearts without cold storage served as control.

ELISA

Mouse hearts without cold storage and those subjected to 6hr-I and subsequent 60 min-reperfusion (6hr-IR) were homogenized in cold RIPA buffer. Supernatant was utilized for analyzing protein levels of TNF-α (DY410), IL-1β (DY401), and HSPA1a (DYC1663) by ELISA based on the manufacturer's instructions (R&D Systems Inc.). All samples and standards were measured in duplicate.

Western Blotting

The heart tissues (without or with 6hr-IR) were lysed in cold RIPA buffer containing Halt protease and phosphatase inhibitor cocktail (ThermoFisher Scientific). The protein extracts (20 μg) from heart tissue were subjected to electrophoresis on a 4-15% Criterion TGX Precast midi protein gel (Bio-Rad, Hercules, CA, USA) and transferred to a PVDF membrane. The membranes were incubated with the following primary antibodies respectively: OXPHOS antibody cocktail (complex I-NDUFB8, complex II-SDHB, complex IV-MTCO1, complex III-UQCRC2, and complex V-ATP5A) (ThermoFisher Scientific), cleaved Caspase-3 (sc-7148) (Santa Cruz Biotechnology Inc., Santa Cruz, CA, USA), and GAPDH (#5174) (Cell Signaling Technology, Beverly, MA, USA), followed by fluorescence-conjugated secondary antibody. The images were detected by a ChemiDoc system (BioRad). Quantification was performed on immunoblotting band density using the Image J software (NIH).

Cell Death by TUNEL Assay

A portion (cross-section) of heart tissue (without or with 6hr-IR) was fixed in 10% buffered formaldehyde, embedded in paraffin, and then sectioned. After paraffin tissue sections were dewaxed, rehydrated, and permeabilized, TUNEL reaction mixture containing terminal deoxynucleotidyl transferase (TdT), fluorescein-dUTP was added to the sections ((DeadEnd Fluorimetric TUNEL System; Promega, Madison, WI). After cell nuclei staining with 4′,6-Diamidino-2-phenylindole (DAPI, blue), images were taken using an Axio Observer

Z1 motorized microscope (Zeiss, Oberchoken, Germany). TUNEL positive cells (apoptotic cells) were counted and represented as the percentage of the nuclei.

Assessment of Hydrogen Peroxide (H_2O_2)

H_2O_2, the most stable form of reactive oxygen species, was measured in heart tissue lysates using a quantitative peroxide assay kit (ThermoFisher Scientific), according to the manufacturer's instructions. All samples and standards were measured in duplicate.

Cold storage experiment on H9c2 cells

The H9c2 rat cardiomyoblast cell line was purchased from the ATCC (Manassas, VA) and cultured in T-75 tissue culture flasks with ATCC-formulated Dulbecco's Modified Eagle's Medium (DMEM) plus 10% of FBS and 1% of Pen-Strep at 37°C, 5% CO_2 and 90% humidity. H9c2 cells were plated in 12-well plate at $1.0X10^5$ cells/well or in 96-well plate at $1.0X10^4$ cells/well. After incubation for 24 hours, media was changed to UW solution containing media vehicle, BM MSC-CM, BM MSC-Exo, or BM MSC-CM^{GW4689} and cells were placed in 0-4°C refrigerator. Six hours later, cells were used for apoptosis detection and mitochondrial membrane potential (MtMP) measurement.

siRNA transfection

Rat Per2 and control siRNA were purchased from Life Technologies. Lipofectamine 2000 (Life Technologies) was used to transfect siRNAs into H9c2 cells based on our previous described method [26, 27]. H9c2 cells were plated in 12-well plate at $1X10^5$/well/ml or in 96-well plate at $1.0X10^4$ cells/well. Twenty fours later, cells were transfected with Per2 or control siRNAs using standard procedure. After one day of transfection, normal H9c2 growth medium was added. The cells were allowed to incubate for an additional one day and used for cold storage experiments as aforementioned.

Determination of apoptosis by flow cytometry

H9c2 cells in different treatment groups were collected from 12-well plate after 6hr cold storage and stained with Annexin-V FITC and propidium iodide (PI) using a Dead Cell Apoptosis kit (ThermoFisher Scientific) according to the manufacturer's protocols. The stained cells were analyzed with a LSR4 flow cytometer (BD Biosciences). Annexin-V was used to detect early apoptotic cells and PI for necrotic or late apoptotic cells. The percentages of cells in different regions (viable cells [Annexin V−/PI−], early apoptotic cells [Annexin V+/PI−], late apoptotic cells [Annexin V+/PI+], and necrotic cells [Annexin V−/PI+]) were determined by Flowjo software. The experiments were repeated four times.

Measurement of Mitochondrial membrane potential

After 6hr cold storage, H9c2 cells in 96-well plate were incubated with a fluorescent probe JC-1 (1 μM, G-Biosciences, St. Louis, MO, USA) at 37°C for 30 minutes. JC-1 goes into mitochondria showing red fluorescence due to formation of dimers/aggregates and is green fluorescence in the cytosol as monomers. After 30-minute incubation, live-cell imaging on H9c2 cells was taken using an Axio Observer Z1 motorized microscope (Zeiss, Oberchoken, Germany) with a 20X objective. In addition, total red (excitation: 535nm; emission: 585nm)

and green (excitation: 485nm; emission: 535nm) fluorescence intensity in each well was obtained using a microplate reader (BioTek). The red to green fluorescence intensity ratio indicates mitochondrial membrane potential.

Statistical Analysis

The reported results were means ± SEM with each dot for individual measurement. Data was checked for variables using Shapiro-Wilk normality test and then analyzed using either student *t*-test or two-way ANOVA with Tukey's post-hoc analysis (detailed information is provided in each figure legend). Difference was considered statistically significant when $p < 0.05$. All statistical analyses were performed using the GraphPad Prism software (GraphPad, La Jolla, CA, USA).

Results

Deep RNA sequencing of myocardial transcriptome profile in mouse hearts under conditions of cold static storage, mimicking clinical scenario for donor heart preservation

To better understand molecular mechanisms underlying myocardial response to cold storage, we first evaluated myocardial transcriptome changes in mouse hearts following 6-hour cold storage/ischemia (6hr-I). Deep RNA sequencing was conducted on mouse hearts without cold storage (baseline control) and stored in UW solution at 0 - 4°C for 6 hours. We identified 266 (FDR<0.1, fold change >=1.5) differentially expressed genes in the 6hr-I hearts compared to baseline control. The complete list of differentially expressed genes are shown in the supplemental materials (Table S1). Using Ingenuity Pathway Analysis (IPA), we also identified the most disrupted canonical pathway as the circadian rhythm signaling (Figure 1A). Within this pathway, several genes including Arntl/Bmal and Per2 in particular, were among those exhibiting the greatest 6hr I-induced deviations from baseline (Figure 1B). The top 10 genes (5 down-regulated and 5 up-regulated) were shown in Figure 1B. In addition, among the top-10 upstream regulators (5 inhibited and 5 activated), the circadian rhythm genes Per2, Per3 and Arntl/Bmal were ranked high as well (Figure 1C). To validate these findings, we detected mRNA levels of Arntl/Bmal and Per2 by RT-qPCR using TaqMan gene expression assay. We observed that the degree of alterations in these two genes' expression was correlated to cold ischemic time with greater deviations from baseline in mouse hearts subjected to longer ischemic time (Figure 1D). The results from human hearts with *ex vivo* cold storage further confirmed changes of transcript levels for Arnt1 and Per2 (Figure 1E). Notably, in addition to circadian clock genes, Hspa1a/1b and TNF were also recognized as top upstream regulators that were upregulated by 6hr-I (Figure 1C). We further identified, among others, dysregulated genes (particularly TNF), which were implicated in modulating mitochondrial performance, oxidative stress response, myocardial function, and apoptosis (Figure 1F).

MSC CM protects the transcriptional integrity of mouse hearts following 6hr cold storage

We next evaluated the beneficial effects of BM-MSC CM and Ad-MSC CM on preserving myocardial transcriptomes in another batch of deep RNA sequencing analysis. In 6hr-I hearts treated with BM-MSC CM or Ad-MSC CM, there were 25 (Table S2) or 42 genes (Table S3) (FDR<0.1, fold change >=1.5) differentially expressed vs. baseline control.

Importantly, for almost all differentially expressed genes by 6hr-I, the degree and direction of change in ischemia vs. baseline control were significantly reversed by the use of BM-MSC CM (Figure 2A, Table S4) or Ad-MSC CM (Figure 2B, Table S3). The correlation showed that on the average, each gene was 24.5% or 22.2% "restored" towards its non-ischemic (normal) value in BM-MSC CM or Ad-MSC CM treated hearts, respectively. Genes increased by 6hr-I were down-regulated by treatment, while genes decreased by ischemia were up-regulated by treatment. Moreover, the use of BM-MSC CM or Ad-MSC CM was able to reverse or improve the dysregulated gene expression (including TNF) involved in circadian pathways, mitochondrial activity, ROS production, left ventricular function, and apoptosis (Figure 2C). These data suggest that either BM-MSC CM or Ad-MSC CM could preserve the normal myocardial transcriptional "fingerprint" despite the ischemic period.

The mechanisms underlying BM-MSC CM or Ad-MSC CM preserved donor hearts during *ex vivo* cold storage

We further compared the efficacy of BM-MSC CM with Ad-MSC CM on myocardial transcriptome preservation following 6hr-I. BM-MSC CM resulted in 284 genes differentially expressed with 67.6% of them downregulated and 32.4% of them upregulated when compared to 6hr-I + vehicle (media control) (Figure 3A, Table S5), while Ad-MSC CM led to 128 genes differentially expressed (59.4% down-regulated and 40.6% up-regulated, Table S6). By using the IPA-based comparative analysis, we identified the top-15 upstream regulators that were activated or inhibited by BM-MSC CM (Figure 3B) and by Ad-MSC CM in the 6hr-I hearts (Figure 3C). The direct comparison between BM-MSC CM and Ad-MSC CM on modulating theses upstream regulators was shown in Figure S5. We noticed that members of inflammatory cytokines and molecules implicated in regulating inflammatory response were the most changed in both treatments, such as proinflammatory cytokines of TNF and IL-1β. Furthermore, the "Disease and Function Analysis" predicted which changes were likely related to 6hr-I induced alterations of gene expression. Interestingly, both BM-MSC CM and Ad-MSC CM could suppress immune cell (including leukocyte, lymphocytes, macrophages, and myeloid cells etc.) movement, migration, recruitment, accumulation, infiltration and activation in 6hr-I mouse hearts (Figure 3D and 3E). Ad-MSC CM seemed to have comparable influence as did BM-MSC CM only on reducing migration and movement of leukocytes among top 25 anticipated alterations of Diseases and Functions based on z-score of BM-MSC CM treatment (Figure 3D). Conversely, BM-MSC CM showed comparable or even better effect on 50% of top 25 predicted changes of Diseases and Functions that were selected on z-score of Ad-MSC CM treatment (Figure 3E). These data suggest that BM-MSC CM may have better effect on inhibiting inflammatory response in the 6hr-I myocardium compared to Ad-MSC CM.

MSC CM protects myocardial function, decreases inflammatory cytokine production, and reduces apoptosis in mouse hearts subjected to 6hr cold storage

Similar to our recent findings [15], 6hr-I significantly impaired myocardial function (Figure 4B, 4D). Notably, either BM-MSC CM or Ad-MSC CM treatment improved LV functional recovery following 6hr cold storage compared to untreated counterparts, as demonstrated by increased LVDP, dP/dt (Figure 4C), and rate pressure product (Figure 4D). However, we did

not observe significant improvement for myocardial diastolic dysfunction in the 6hr-I hearts treated with MSC secretome (Figure 4C).

Considering that 6hr-I leads to differentially expressed inflammatory genes and apoptotic-related genes, we evaluated the effect of MSC secretome on regulating myocardial inflammatory cytokine production and apoptosis in isolated mouse hearts following 6hr-I and 60-min reperfusion (6hr-IR). BM-MSC CM significantly reduced myocardial production of TNF-α, IL-1β and Hspa1a (Figure 5A), while Ad-MSC CM markedly decreased myocardial TNF-α production. We also found 6hr-IR significantly increased cleaved/active caspase-3 level (Figure 5B). Using MSC-CM (either BM or Ad) protected the myocardium against 6hr-IR, as shown by decreased cleaved/active caspase-3 levels compared to the untreated 6hr-IR group (Figure 5B). Importantly, the TUNEL assay confirmed that 6hr-IR resulted in more apoptotic cells in myocardium, which was significantly reduced by treatment with BM-MSC CM and Ad-MSC CM (Figure 5C and 5D). These findings suggest that MSC secretome is able to suppress 6hr-IR induced inflammatory cytokine production and apoptosis, thus protecting mouse hearts from cold ischemic damage and subsequent reperfusion injury.

The effect of MSC CM on oxidative metabolism

The 6hr-I led to differentially expressed genes that were implicated in modulating mitochondrial function and oxidative stress response (Figure 1D), while BM- and Ad-MSC CM restored or improved these gene expression (Figure 2C). Therefore, we investigated myocardial levels of H_2O_2 production and mitochondrial oxidative phosphorylation (OXPHOS) complex proteins. We found that MSC CM significantly reduced H_2O_2 production in 6hr-IR hearts (Figure 6A), suggesting that MSC secretome could improve myocardial recovery by reducing oxidative stress in donor hearts following *ex vivo* cold storage. Additionally, Western blot analysis indicated a trend of decreased protein levels of complex II-SDHB and complex IV-MTCO1 in mouse hearts following 6hr-IR (Figure 6B and 6C). Ad-MSC CM significantly restored myocardial levels of complex II-SDHB and complex IV-MTCO1 (Figure 6C). Despite a trend of increased OXPHOS protein levels in BM-MSC CM treated hearts compared to the 6hr-IR group, we did not notice statistical differences.

Components of MSC secretome in improving cell survival and mitochondrial preservation during cold storage

Soluble factors (growth factors, chemokines, cytokines etc.) and exosomes/extracellular vesicles (Exo) are major components in MSC secretome. To evaluate which components (soluble factors vs. exosomes) are more responsible for MSC-mediated myocardial preservation following cold storage, we determined active caspase-3 levels in mouse hearts subjected to 6hr-I, 6hr-I+MSC-CM, 6hr-I+MSC-Exo, and 6hr-I+MSC-CM^{GW4869} (exosome-depleted CM). Exosome preparation from BM-MSC culture was validated by exosomal marker CD63 expression (Figure S6A), morphology (Figure S6B), and size distribution (Figure S6C). Of note, 6hr cold storage without reperfusion significantly increased pro-apoptotic signal of active caspase-3 expression in isolated mouse hearts, whereas BM-MSC CM decreased myocardial levels of cleaved caspase-3 (Figure 7A and

7B). However, we did not observe markedly reduced cleaved caspase-3 in MSC-Exo or exosome-depleted CM (either one from culturing same cell numbers as MSC CM did) treated group (Figure 7A and 7B). To further explore the effect of MSC secretome components on 6hr cold storage-induced apoptosis, we utilized H9c2 cardiac myoblasts. Significantly increased apoptosis (both early and late) was noticed in H9c2 cells subjected to 6hr cold storage (Figure 7C–7E). Using BM-MSC CM in UW solution decreased 6hr I-induced apoptosis, but not necrosis (Figure 7C and 7D). However, either BM MSC-Exo or BM MSC-CM^{GW4869} alone did not convey anti-apoptotic effect on H9c2 cells following cold ischemia (Figure 7E). The most of cells (> 98%) were gated in flow cytometric analysis (Figure S7).

Furthermore, mitochondrial membrane potential (MtMP) plays critical roles in maintaining mitochondrial function and health, as well as in apoptosis induction. Therefore, we determined the effect of MSC-CM, MSC-Exo, and MSC-CM^{GW4869} on MtMP in living H9c2 cells after 6hr cold storage. Reduced MtMP was observed in 6hr -treated H9c2 cells compared to their control counterparts (Figure 7F and 7G). BM-MSC CM significantly preserved MtMP in 6hr I-impaired H9c2 cells, but not BM MSC-Exo or BM MSC-CM^{GW4869} alone (Figure 7F and 7G).

The effect of myocardial Per2 expression in MSC CM-mediated cardiomyocyte preservation following cold storage

Our deep RNA sequencing data identified that Per2 was one of the top differentially expressed genes in mouse heart induced by 6hr cold storage. We therefore investigated myocardial Per2 expression among groups of no cold storage (control), 6hr-I, 6hr-I+MSC-CM, 6hr-I+MSC-Exo, and 6hr-I+MSC-CM^{GW4869}. We observed that 6hr cold storage significantly decreased myocardial Per2 levels (both mRNA and protein), whereas BM-MSC CM restored its levels (Figure 8A–8C). To determine the role of myocardial Per2 expression in MSC CM-mediated paracrine protein following cold ischemia, we next used siRNA to specifically suppress the expression of Per2 in H9c2 cells (rat cardiomyoblast cell line). Per2 expression was significantly decreased in H9c2 cells transfected with Per2 siRNA compared with the cells treated with control siRNA (Figure 8D, 8E). Interestingly, knockdown of Per2 abolished BM-MSC CM-mediated anti-apoptosis in H9c2 cells subjected to 6hr cold storage (Figure 8F and 8G), while significantly reduced apoptosis was in MSC CM-treated H9c2 cells with control siRNA transfection (Figure S8). Furthermore, BM-MSC CM was noticed to preserve MtMP in H9c2 cells transfected with control siRNA (Figure S9). However, suppression of Per2 expression neutralized MSC CM-derived protection of MtMP (Figure 8H and 8I).

Discussion

During organ procurement, cardiac arrest is instantly introduced by infusion of cold cardioplegia solution following aortic cross-clamping to lower the heart's metabolism. However, cardiac metabolic rate does not drop to zero while its supply of oxygen and nutrients is cut-off, resulting in ischemic damage. Ischemic time of donor hearts is a critical determinant to impact transplant outcome. Short ischemia periods during safe cold storage

do not cause the heart major problems, but challenges occur with time beyond 4 hours. It has been shown that recipient survival decreases with increased ischemic time of donor heart, especially for storage >4-6 hours [28, 29]. While prolonged storage could provide more organs, it would increase the extent of ischemia. Therefore, it is critical to understand molecular mechanisms underlying pathophysiological process of donor hearts when storage time > 4hr.

The dynamic changes of myocardial transcriptome expression profile occur in LV tissue with an average period of 79 minutes during cold cardioplegic arrest in patients who underwent cardiopulmonary bypass [30]. However, such observation obtained from already injured myocardium may not be informative and practical for directing clinical heart transplantation. In this study, we provided the comprehensive understanding of myocardial transcriptome profile alterations in mouse hearts following 6hr cold storage. The deep RNA-sequencing analysis has shown that 6hr-I resulted in differentially expressed genes in inflammatory response, mitochondrial activity, oxidative stress response, LV function, and apoptosis. These findings were in line with the observations from a recent study, in which the most pronounced transcriptomic alterations were observed in pathways of inflammation, oxidative phosphorylation and cell death in human LV after 8hr cold storage [31].

Of note, our deep RNA sequencing data identified that the circadian rhythm signaling was the most disrupted canonical pathway in mouse hearts following 6hr cold ischemia. The circadian clock is a molecular oscillator driven by light/dark cycles and the clock genes not only regulate physiological rhythms, but also participate in fundamental physiological processes, such as energy metabolism. Emerging studies have indicated that the function of clock genes affects mitochondrial energy production via regulating mitochondrial respiratory cycles [32, 33]. Specifically, the clock regulators Arntl/Bam1 and Per2 have been reported to impact mitochondrial performance. Cardiac-specific deletion of Arntl/Bmal1 in mice results in cardiac mitochondrial defects, thus leading to reduced cardiac function with age [34]. Per2 is shown to control mitochondrial oxidative metabolism in mouse myoblasts when exposed to fatty acid oxidation [33]. Altered mitochondrial morphology and activity have also been observed in Per2 knockout mice following myocardial ischemia [35, 36]. Our present study provides the first evidence showing that Arntl/Bmal1 and Per2 are not only top differentially expressed genes, but also high ranked upstream regulators to modulate myocardial biological response to cold ischemia. The results from human heart samples also confirmed that 6hr-cold storage led to myocardial alterations of Arntl/Bmal1 and Per2.

In addition to being regulated by circadian rhythms, external stimuli (ionizing radiation, UV light, etc.) affect Per2 gene expression [37]. Heat shock factor 1 (HSF1), a stress related gene, is shown to induce Per2 in the brown adipose tissue [38]. TNF-α is also reported to suppress Per2 expression in NIH 3T3 fibroblast [39]. On the other hand, molecules and signaling pathways that impact Per2 protein stability contribute to Per2 protein levels as well. The stress kinase mitogen-activated protein kinase kinase 7 (MKK7)-mediated JNK activation has been demonstrated to increase the half-life of Per2 protein [40]. In current study, we did see changes of TNF-α expression (but not HSF1 or MKK7 via deep RNA sequencing data analysis) by cold ischemia or MSC CM, suggesting that alteration of myocardial Per2 levels may be a secondary response to cold storage-increased

or MSC CM-reduced TNF-α. Using siRNA to specifically knockdown Per2 expression neutralized MSC CM-mediated anti-apoptosis and MSC CM-preserved MtMP in response to 6hr cold ischemia in present study, indicating an important role of myocardial Per2 in MSC-mediated paracrine protection. Nevertheless, further investigations are required to evaluate the roles of the clock genes in regulating mitochondrial performance, metabolic function, and inflammatory response in donor hearts following cold storage.

On the other hand, stress including ischemia induces expression of Hspa1a and Hspa1b, two inducible members of the 70-kDa family of heat shock protein (Hsp70). Notably, Hsp70 has been studied in heart failure and myocardial I/R for years [41]. The increased Hsp70 is observed in patients with myocardial ischemia, unstable angina and open-heart surgery [42, 43]. Therefore, Hsp70 may be used as a biomarker for the presence of heart failure caused by cardiomyopathies of different etiologies [44] and may act as a potential clinical marker for heart failure at early stage [45]. In fact, increased circulating (extracellular) levels of Hsp70 relate to severity of heart failure [46] and exhibit a moderate positive correlation with IL-6, IL-8, and TNF-α [46]. Circulating Hsp70 has also been shown to induce inflammatory cytokine production through toll-like receptor 4 or 2 following myocardial ischemia [43, 47–49]. In this study, the RNA-seq analysis identified myocardial Hspa1a/1b among top 3 genes upregulated by 6hr cold storage and as the top upstream regulator with activation by 6hr cold storage. Significantly increased Hspa1a levels were further noticed in mouse hearts with 6hr-IR compared to no cold storage group. Collectively, our findings extend the role of Hspa1a and Hspa1b in heart failure and myocardial I/R to donor heart underwent cold storage, and suggest their levels may indicate the degree of myocardial damage along with cold ischemia. However, future studies are needed to identify the possibility of Hspa1a/1b as potential biomarkers showing early myocardial damage in heart transplantation.

When donor heart is re-implanted into a recipient, reperfusion occurs and it can aggravate ischemic damage. I/R injury is inevitable in heart transplantation and is a critical factor to influence graft function and clinical outcome after organ transplantation. Therefore, modification of the organ preservation solution to ameliorate pre-transplant I/R injury of donor hearts and to prolong preservation time (thus increasing organ exchange across distant geographical areas) is particularly attractive. In this study, adding MSC-derived secretome (either from BM-MSC or Ad-MSC) to preservation solution protected cold ischemia-induced myocardial transcriptome changes in donor hearts. Specifically, they restored differentially expressed genes involved in inflammatory response, mitochondrial activity, oxidative stress response, LV function, and apoptosis towards normal condition. In line with these, we found that BM-MSC CM and Ad-MSC CM significantly improved myocardial functional recovery in 6hr-I mouse hearts compared to untreated counterparts. In addition, myocardial production of inflammatory cytokines (TNFα and IL-1β) and Hspa1a was decreased in MSC CM-treated hearts following 6hr-I and subsequent resuscitation. Reduced apoptosis was further observed in MSC CM treated mouse hearts.

MSC secretome contains multiple protective soluble factors and exosomes/extracellular vesicles. We have previously shown that MSCs produce substantial amount of VEGF, HGF, and SDF-1 [4, 5, 22, 50, 51], which are well defined for their effects on angiogenesis and anti-apoptosis [3, 22, 51–53]. Additionally, exosomes have emerged as essential components

of the MSC secretome to mediate protective effects [15, 54–56]. In present study, we evaluated whether soluble factors (exosome-depleted CM) or exosomes are accountable for MSC CM-mediated donor heart preservation during cold storage. Unexpectedly, either MSC-Exo or exosome-depleted CM did not convey protection of MSC secretome on cell survival and MtMP in response to 6hr cold storage, suggesting that MSC-derived trophic factors and exosomes likely synergize to provide protective activity in donor hearts against cold ischemia. Also, it is possible that the degree of injury is moderate without reperfusion so as not to see beneficial effects of MSC-Exo and exosome-depleted CM. Furthermore, the dosage of MSC-Exo or exosome-depleted CM may not be appropriate to achieve significant protection in this study.

Mitochondrial dysfunction is one of the important cardiac toxicity pathways interrupted by cold ischemia (Figure 1A), correlated with the disrupted gene transcription for mitochondrial complex I and mitochondrial uncoupling protein in mouse hearts. In addition to this, we noticed a trend of decreased mitochondrial respiratory chain proteins complex II-SDHB and complex IV-MTCO1 in mouse hearts subjected to 6hr-IR. This possible reduction of mitochondrial oxidative phosphorylation is in line with findings of downregulation of oxidative phosphorylation pathway as one of most changed transcriptomic profile in human LV subjected to 8hr cold storage [31]. Notably, a loss-of-function mutation of the transhydrogenase (Nnt) gene (due to the missense of exons 7 – 11) exists in C57BL/6 mice from the Jackson Laboratories (C57BL/6J) [57] and this missense of a functional Nnt has shown to reduce oxidative stress and cell death, and improve LV function in C57BL/6J mice following pressure overload [58]. Thus, it is unclear whether the use of C57BL/6J mice led to cardiac protection with mild changes of mitochondrial oxidative phosphorylation pathways following 6hr cold storage in present study, and requires further investigation using different mouse strains in the future.

MSC CM appeared to restore myocardial levels of five OXPHOS proteins that were evaluated in this study. However, we need to point out that there were no statistical differences in mitochondrial OXPHOS complex protein levels among groups (except Ad-MSC CM vs. 6hr-IR in two proteins). A possible explanation about this could be that the optimum time period was missed for evaluating changes of OXPHOS proteins due to only one-time point used in this study. Also, we found that BM-MSC CM significantly reduced myocardial production of H_2O_2 compared to vehicle group. Collectively, these findings suggested that MSC secretome played a role in preserving oxidative phosphorylation pathways in donor hearts following cold ischemic storage. In fact, emerging evidence has shown that the MSC secretome could modify cardiac metabolism. The myocardial bioenergetic improvements have been observed in the infarct border zone with MSC transplantation, which are most likely secondary to MSC-mediated paracrine effect [59]. In addition, modified MSCs with Akt overexpression preserve normal metabolism in the surviving myocardium following myocardial infarction [60]. Our current study further indicated that MSC secretome improved cardiomyocyte mitochondrial membrane potential in response to cold ischemia, suggesting the role of MSC paracrine action in maintaining mitochondrial health and thus preserving normal metabolic status during myocardial injury.

Although similar mechanisms were noticed underlying BM-MSC CM- and Ad-MSC CM-protected donor hearts following cold ischemia, there were also a few differences between these two treatments. BM-MSC CM seemed to have greater effects on preserving 6hr-I-altered myocardial transcriptome profile in inflammatory cytokines and in inflammatory response compared to Ad-MSC CM. With respect to how this disparity happened, it is possible that different secretome patterns exist between BM-MSC CM and Ad-MSC CM. In fact, it is suggested that MSCs from different sources may have different secretion potentials and patterns [61–63]. A recent study on profiling of MSC secretome has proved this notion that there were 24.1% of human proteins in BM-MSC secretome and 27.5% in Ad-MSC secretome different, along with more than 72% identified in both [64]. In addition, differences in miRNA expression profiles (~30%) have also been identified in BM-MSC and Ad-MSC derived exosomes that were contained in MSC secretome [65]. Albeit these differences, our data here support the protective effects of both MSC secretome in donor hearts during cold ischemia storage.

In summary, the present study clearly showed that 6hr cold storage caused alterations of myocardial transcriptome profile. Among these, mitochondrial injury, dysregulated inflammatory response and oxidative stress response, as well as apoptosis, have been identified, along with depression of myocardial function. Importantly, MSC secretome from BM-MSCs and Ad-MSCs could restore or improve 6hr-I induced myocardial transcriptome changes towards normal status, thus ameliorating pre-transplant cold ischemic injury in donor hearts during their storage and promoting graft functional recovery (Figure 9). Furthermore, myocardial Per2 might play an important role in MSC secretome-mediated cardiac preservation during cold storage. Our results provide particularly valued evidence for the use of cell-free, secretome-based therapies to optimize current standard storage solution, thereby improving recipient outcomes post transplantation.

Supplementary Material

Refer to Web version on PubMed Central for supplementary material.

Acknowledgements:

The RNA-Sequencing studies were carried out in the Center for Medical Genomics at Indiana University School of Medicine (IUSM). The sequencing data alignment was processed by the Center for Computational Biology and Bioinformatics at Indiana University. We thank Mrs. Caroline Miller from the Electron Microscopy Center at IUSM for her technical assistance in acquiring transmission electron microscopy image. We also thank Dr. Teresa A. Zimmers at IUSM for allowing access to the equipment for taking fluorescent images.

Funding:

This study is partially supported by the Methodist Health Foundation (to IW & MW), by National Institutes of Health (NIH) R56 HL139967 (to MW), by the Indiana Clinical and Translational Sciences Institute via a Project Development Team pilot grant (UL1TR001108), and by a Veterans Affairs Merit Review grant (I01 BX003888 to KLM). The content is solely the responsibility of the authors and does not necessarily represent the official views of the funding agencies.

References

[1]. Colvin M, Smith JM, Hadley N, Skeans MA, Uccellini K, Goff R, et al. OPTN/SRTR 2018 Annual Data Report: Heart, Am J Transplant 2020;20 Suppl s1 340–426. [PubMed: 31898418]

[2]. Zaroff JG, Rosengard BR, Armstrong WF, Babcock WD, D'Alessandro A, Dec GW, et al. Consensus conference report: maximizing use of organs recovered from the cadaver donor: cardiac recommendations, March 28-29, 2001, Crystal City, Va, Circulation 2002;106(7): 836–41. [PubMed: 12176957]

[3]. Wang M, Tan J, Wang Y, Meldrum KK, Dinarello CA, Meldrum DR, IL-18 binding protein-expressing mesenchymal stem cells improve myocardial protection after ischemia or infarction, Proc Natl Acad Sci U S A 2009;106(41): 17499–504. [PubMed: 19805173]

[4]. Wang M, Crisostomo PR, Herring C, Meldrum KK, Meldrum DR, Human progenitor cells from bone marrow or adipose tissue produce VEGF, HGF, and IGF-I in response to TNF by a p38 MAPK-dependent mechanism, Am J Physiol Regul Integr Comp Physiol 2006;291(4): R880–4. [PubMed: 16728464]

[5]. Rehman J, Traktuev D, Li J, Merfeld-Clauss S, Temm-Grove CJ, Bovenkerk JE, et al. Secretion of angiogenic and antiapoptotic factors by human adipose stromal cells, Circulation 2004;109(10): 1292–8. [PubMed: 14993122]

[6]. Gnecchi M, He H, Liang OD, Melo LG, Morello F, Mu H, et al. Paracrine action accounts for marked protection of ischemic heart by Akt-modified mesenchymal stem cells, Nat Med 2005;11(4): 367–8. [PubMed: 15812508]

[7]. Zuo S, Jones WK, Li H, He Z, Pasha Z, Yang Y, et al. Paracrine effect of Wnt11-overexpressing mesenchymal stem cells on ischemic injury, Stem Cells Dev 2012;21(4): 598–608. [PubMed: 21463175]

[8]. Madonna R, Angelucci S, Di Giuseppe F, Doria V, Giricz Z, Gorbe A, et al. Proteomic analysis of the secretome of adipose tissue-derived murine mesenchymal cells overexpressing telomerase and myocardin, J Mol Cell Cardiol 2019;131 171–186. [PubMed: 31055035]

[9]. Suncion VY, Ghersin E, Fishman JE, Zambrano JP, Karantalis V, Mandel N, et al. Does transendocardial injection of mesenchymal stem cells improve myocardial function locally or globally?: An analysis from the Percutaneous Stem Cell Injection Delivery Effects on Neomyogenesis (POSEIDON) randomized trial, Circ Res 2014;114(8): 1292–301. [PubMed: 24449819]

[10]. Heldman AW, DiFede DL, Fishman JE, Zambrano JP, Trachtenberg BH, Karantalis V, et al. Transendocardial mesenchymal stem cells and mononuclear bone marrow cells for ischemic cardiomyopathy: the TAC-HFT randomized trial, JAMA 2014;311(1): 62–73. [PubMed: 24247587]

[11]. Ward MR, Abadeh A, Connelly KA, Concise Review: Rational Use of Mesenchymal Stem Cells in the Treatment of Ischemic Heart Disease, Stem Cells Transl Med 2018;7(7): 543–550. [PubMed: 29665255]

[12]. Samper E, Diez-Juan A, Montero JA, Sepulveda P, Cardiac cell therapy: boosting mesenchymal stem cells effects, Stem Cell Rev Rep 2013;9(3): 266–80. [PubMed: 22350458]

[13]. Cashman TJ, Gouon-Evans V, Costa KD, Mesenchymal stem cells for cardiac therapy: practical challenges and potential mechanisms, Stem Cell Rev Rep 2013;9(3): 254–65. [PubMed: 22577007]

[14]. Korkmaz-Icoz S, Li S, Huttner R, Ruppert M, Radovits T, Loganathan S, et al. Hypothermic perfusion of donor heart with a preservation solution supplemented by mesenchymal stem cells, J Heart Lung Transplant 2019;38(3): 315–326. [PubMed: 30638838]

[15]. Wang M, Yan L, Li Q, Yang Y, Turrentine M, March K, et al. Mesenchymal stem cell secretions improve donor heart function following ex vivo cold storage, J Thorac Cardiovasc Surg 2020.

[16]. Ellis BW, Traktuev DO, Merfeld-Clauss S, Can UI, Wang M, Bergeron R, et al. Adipose stem cell secretome markedly improves rodent heart and human induced pluripotent stem cell-derived cardiomyocyte recovery from cardioplegic transport solution exposure, Stem Cells 2021;39(2): 170–182. [PubMed: 33159685]

[17]. Wang L, Gu H, Turrentine M, Wang M, Estradiol treatment promotes cardiac stem cell (CSC)-derived growth factors, thus improving CSC-mediated cardioprotection after acute ischemia/reperfusion, Surgery 2014;156(2): 243–52. [PubMed: 24957669]

[18]. Kosaka N, Iguchi H, Yoshioka Y, Takeshita F, Matsuki Y, Ochiya T, Secretory mechanisms and intercellular transfer of microRNAs in living cells, J Biol Chem 2010;285(23): 17442–52. [PubMed: 20353945]

[19]. Singh K, Pal D, Sinha M, Ghatak S, Gnyawali SC, Khanna S, et al. Epigenetic Modification of MicroRNA-200b Contributes to Diabetic Vasculopathy, Mol Ther 2017;25(12): 2689–2704. [PubMed: 29037594]

[20]. Singh K, Sinha M, Pal D, Tabasum S, Gnyawali SC, Khona D, et al. Cutaneous Epithelial to Mesenchymal Transition Activator ZEB1 Regulates Wound Angiogenesis and Closure in a Glycemic Status-Dependent Manner, Diabetes 2019;68(11): 2175–2190. [PubMed: 31439646]

[21]. Wisler JR, Singh K, McCarty AR, Abouhashem ASE, Christman JW, Sen CK, Proteomic Pathway Analysis of Monocyte-Derived Exosomes during Surgical Sepsis Identifies Immunoregulatory Functions, Surg Infect (Larchmt) 2020;21(2): 101–111. [PubMed: 31478785]

[22]. Huang C, Gu H, Yu Q, Manukyan MC, Poynter JA, Wang M, Sca-1+ cardiac stem cells mediate acute cardioprotection via paracrine factor SDF-1 following myocardial ischemia/reperfusion, PLoS One 2011;6(12): e29246. [PubMed: 22195033]

[23]. Wang M, Crisostomo PR, Markel TA, Wang Y, Meldrum DR, Mechanisms of sex differences in TNFR2-mediated cardioprotection, Circulation 2008;118(14 Suppl): S38–45. [PubMed: 18824767]

[24]. Wang M, Crisostomo P, Wairiuko GM, Meldrum DR, Estrogen receptor-alpha mediates acute myocardial protection in females, Am J Physiol Heart Circ Physiol 2006;290(6): H2204–9. [PubMed: 16415070]

[25]. Wang M, Wang Y, Weil B, Abarbanell A, Herrmann J, Tan J, et al. Estrogen receptor beta mediates increased activation of PI3K/Akt signaling and improved myocardial function in female hearts following acute ischemia, Am J Physiol Regul Integr Comp Physiol 2009;296(4): R972–8. [PubMed: 19211725]

[26]. Huang C, Gu H, Zhang W, Manukyan MC, Shou W, Wang M, SDF-1/CXCR4 mediates acute protection of cardiac function through myocardial STAT3 signaling following global ischemia/reperfusion injury, Am J Physiol Heart Circ Physiol 2011;301(4): H1496–505. [PubMed: 21821779]

[27]. Wang M, Yu Q, Wang L, Gu H, Distinct patterns of histone modifications at cardiac-specific gene promoters between cardiac stem cells and mesenchymal stem cells, Am J Physiol Cell Physiol 2013;304(11): C1080–90. [PubMed: 23552285]

[28]. Young JB, Hauptman PJ, Naftel DC, Ewald G, Aaronson K, Dec GW, et al. Determinants of early graft failure following cardiac transplantation, a 10-year, multi-institutional, multivariable analysis, J Heart Lung Transplant 2001;20(2): 212.

[29]. Johnson MR, Meyer KH, Haft J, Kinder D, Webber SA, Dyke DB, Heart transplantation in the United States, 1999-2008, Am J Transplant 2010;10(4 Pt 2): 1035–46. [PubMed: 20420651]

[30]. Muehlschlegel JD, Christodoulou DC, McKean D, Gorham J, Mazaika E, Heydarpour M, et al. Using next-generation RNA sequencing to examine ischemic changes induced by cold blood cardioplegia on the human left ventricular myocardium transcriptome, Anesthesiology 2015;122(3): 537–50. [PubMed: 25581909]

[31]. Lei I, Wang Z, Chen YE, Ma PX, Huang W, Kim E, et al. “The Secret Life of Human Donor Hearts”: An Examination of Transcriptomic Events During Cold Storage, Circ Heart Fail 2020;13(4): e006409. [PubMed: 32264717]

[32]. Woldt E, Sebti Y, Solt LA, Duhem C, Lancel S, Eeckhoute J, et al. Rev-erb-alpha modulates skeletal muscle oxidative capacity by regulating mitochondrial biogenesis and autophagy, Nat Med 2013;19(8): 1039–46. [PubMed: 23852339]

[33]. Peek CB, Affinati AH, Ramsey KM, Kuo HY, Yu W, Sena LA, et al. Circadian clock NAD+ cycle drives mitochondrial oxidative metabolism in mice, Science 2013;342(6158): 1243417. [PubMed: 24051248]

[34]. Kohsaka A, Das P, Hashimoto I, Nakao T, Deguchi Y, Gouraud SS, et al. The circadian clock maintains cardiac function by regulating mitochondrial metabolism in mice, PLoS One 2014;9(11): e112811. [PubMed: 25389966]

[35]. Eckle T, Hartmann K, Bonney S, Reithel S, Mittelbronn M, Walker LA, et al. Adora2b-elicited Per2 stabilization promotes a HIF-dependent metabolic switch crucial for myocardial adaptation to ischemia, Nat Med 2012;18(5): 774–82. [PubMed: 22504483]

[36]. Virag JA, Anderson EJ, Kent SD, Blanton HD, Johnson TL, Moukdar F, et al. Cardioprotection via preserved mitochondrial structure and function in the mPer2-mutant mouse myocardium, Am J Physiol Heart Circ Physiol 2013;305(4): H477–83. [PubMed: 23771689]

[37]. Fu L, Pelicano H, Liu J, Huang P, Lee C, The circadian gene Period2 plays an important role in tumor suppression and DNA damage response in vivo, Cell 2002;111(1): 41–50. [PubMed: 12372299]

[38]. Chappuis S, Ripperger JA, Schnell A, Rando G, Jud C, Wahli W, et al. Role of the circadian clock gene Per2 in adaptation to cold temperature, Mol Metab 2013;2(3): 184–93. [PubMed: 24049733]

[39]. Cavadini G, Petrzilka S, Kohler P, Jud C, Tobler I, Birchler T, et al. TNF-alpha suppresses the expression of clock genes by interfering with E-box-mediated transcription, Proc Natl Acad Sci U S A 2007;104(31): 12843–8. [PubMed: 17646651]

[40]. Uchida Y, Osaki T, Yamasaki T, Shimomura T, Hata S, Horikawa K, et al. Involvement of stress kinase mitogen-activated protein kinase kinase 7 in regulation of mammalian circadian clock, J Biol Chem 2012;287(11): 8318–26. [PubMed: 22267733]

[41]. Kim YK, Suarez J, Hu Y, McDonough PM, Boer C, Dix DJ, et al. Deletion of the inducible 70-kDa heat shock protein genes in mice impairs cardiac contractile function and calcium handling associated with hypertrophy, Circulation 2006;113(22): 2589–97. [PubMed: 16735677]

[42]. Valen G, Hansson GK, Dumitrescu A, Vaage J, Unstable angina activates myocardial heat shock protein 72, endothelial nitric oxide synthase, and transcription factors NFkappaB and AP-1, Cardiovasc Res 2000;47(1): 49–56. [PubMed: 10869529]

[43]. Dybdahl B, Wahba A, Lien E, Flo TH, Waage A, Qureshi N, et al. Inflammatory response after open heart surgery: release of heat-shock protein 70 and signaling through toll-like receptor-4, Circulation 2002;105(6): 685–90. [PubMed: 11839622]

[44]. Wei YJ, Huang YX, Shen Y, Cui CJ, Zhang XL, Zhang H, et al. Proteomic analysis reveals significant elevation of heat shock protein 70 in patients with chronic heart failure due to arrhythmogenic right ventricular cardiomyopathy, Mol Cell Biochem 2009;332(1-2): 103–11. [PubMed: 19543852]

[45]. Li Z, Song Y, Xing R, Yu H, Zhang Y, Li Z, et al. Heat shock protein 70 acts as a potential biomarker for early diagnosis of heart failure, PLoS One 2013;8(7): e67964. [PubMed: 23874478]

[46]. Genth-Zotz S, Bolger AP, Kalra PR, von Haehling S, Doehner W, Coats AJ, et al. Heat shock protein 70 in patients with chronic heart failure: relation to disease severity and survival, Int J Cardiol 2004;96(3): 397–401. [PubMed: 15301893]

[47]. Zou N, Ao L, Cleveland JC Jr., Yang X, Su X, Cai GY, et al. Critical role of extracellular heat shock cognate protein 70 in the myocardial inflammatory response and cardiac dysfunction after global ischemia-reperfusion, Am J Physiol Heart Circ Physiol 2008;294(6): H2805–13. [PubMed: 18441202]

[48]. Ao L, Zou N, Cleveland JC Jr., Fullerton DA, Meng X, Myocardial TLR4 is a determinant of neutrophil infiltration after global myocardial ischemia: mediating KC and MCP-1 expression induced by extracellular HSC70, Am J Physiol Heart Circ Physiol 2009;297(1): H21–8. [PubMed: 19448144]

[49]. Mathur S, Walley KR, Wang Y, Indrambarya T, Boyd JH, Extracellular heat shock protein 70 induces cardiomyocyte inflammation and contractile dysfunction via TLR2, Circ J 2011;75(10): 2445–52. [PubMed: 21817814]

[50]. Wang M, Zhang W, Crisostomo P, Markel T, Meldrum KK, Fu XY, et al. STAT3 mediates bone marrow mesenchymal stem cell VEGF production, J Mol Cell Cardiol 2007;42(6): 1009–15. [PubMed: 17509611]

[51]. Cai L, Johnstone BH, Cook TG, Liang Z, Traktuev D, Cornetta K, et al. Suppression of hepatocyte growth factor production impairs the ability of adipose-derived stem cells to promote ischemic tissue revascularization, Stem Cells 2007;25(12): 3234–43. [PubMed: 17901400]

[52]. Wang Y, Haider HK, Ahmad N, Xu M, Ge R, Ashraf M, Combining pharmacological mobilization with intramyocardial delivery of bone marrow cells over-expressing VEGF is more effective for cardiac repair, J Mol Cell Cardiol 2006;40(5): 736–45. [PubMed: 16603183]

[53]. Haider H, Jiang S, Idris NM, Ashraf M, IGF-1-overexpressing mesenchymal stem cells accelerate bone marrow stem cell mobilization via paracrine activation of SDF-1alpha/CXCR4 signaling to promote myocardial repair, Circ Res 2008;103(11): 1300–8. [PubMed: 18948617]

[54]. Lai RC, Arslan F, Lee MM, Sze NS, Choo A, Chen TS, et al. Exosome secreted by MSC reduces myocardial ischemia/reperfusion injury, Stem Cell Res 2010;4(3): 214–22. [PubMed: 20138817]

[55]. Baglio SR, Pegtel DM, Baldini N, Mesenchymal stem cell secreted vesicles provide novel opportunities in (stem) cell-free therapy, Front Physiol 2012;3 359. [PubMed: 22973239]

[56]. Eirin A, Riester SM, Zhu XY, Tang H, Evans JM, O'Brien D, et al. MicroRNA and mRNA cargo of extracellular vesicles from porcine adipose tissue-derived mesenchymal stem cells, Gene 2014;551(1): 55–64. [PubMed: 25158130]

[57]. Toye AA, Lippiat JD, Proks P, Shimomura K, Bentley L, Hugill A, et al. A genetic and physiological study of impaired glucose homeostasis control in C57BL/6J mice, Diabetologia 2005;48(4): 675–86. [PubMed: 15729571]

[58]. Nickel AG, von Hardenberg A, Hohl M, Loffler JR, Kohlhaas M, Becker J, et al. Reversal of Mitochondrial Transhydrogenase Causes Oxidative Stress in Heart Failure, Cell Metab 2015;22(3): 472–84. [PubMed: 26256392]

[59]. Feygin J, Mansoor A, Eckman P, Swingen C, Zhang J, Functional and bioenergetic modulations in the infarct border zone following autologous mesenchymal stem cell transplantation, Am J Physiol Heart Circ Physiol 2007;293(3): H1772–80. [PubMed: 17573463]

[60]. Gnecchi M, He H, Melo LG, Noiseaux N, Morello F, de Boer RA, et al. Early beneficial effects of bone marrow-derived mesenchymal stem cells overexpressing Akt on cardiac metabolism after myocardial infarction, Stem Cells 2009;27(4): 971–9. [PubMed: 19353525]

[61]. Strioga M, Viswanathan S, Darinskas A, Slaby O, Michalek J, Same or not the same? Comparison of adipose tissue-derived versus bone marrow-derived mesenchymal stem and stromal cells, Stem Cells Dev 2012;21(14): 2724–52. [PubMed: 22468918]

[62]. Izadpanah R, Trygg C, Patel B, Kriedt C, Dufour J, Gimble JM, et al. Biologic properties of mesenchymal stem cells derived from bone marrow and adipose tissue, J Cell Biochem 2006;99(5): 1285–97. [PubMed: 16795045]

[63]. Noel D, Caton D, Roche S, Bony C, Lehmann S, Casteilla L, et al. Cell specific differences between human adipose-derived and mesenchymal-stromal cells despite similar differentiation potentials, Exp Cell Res 2008;314(7): 1575–84. [PubMed: 18325494]

[64]. Shin S, Lee J, Kwon Y, Park KS, Jeong JH, Choi SJ, et al. Comparative Proteomic Analysis of the Mesenchymal Stem Cells Secretome from Adipose, Bone Marrow, Placenta and Wharton's Jelly, Int J Mol Sci 2021;22(2).

[65]. Baglio SR, Rooijers K, Koppers-Lalic D, Verweij FJ, Perez Lanzon M, Zini N, et al. Human bone marrow- and adipose-mesenchymal stem cells secrete exosomes enriched in distinctive miRNA and tRNA species, Stem Cell Res Ther 2015;6 127. [PubMed: 26129847]

Highlights

- MSC secretome preserves normal transcriptional profiling in hearts with cold storage
- MSC's origin is not a key determinant for MSC secretome-derived protective effect
- MSC-trophic factors and exosomes synergistically act for donor heart preservation
- Knockdown of Per2 abolishes MSC secretome-mediated protective activity in myocytes

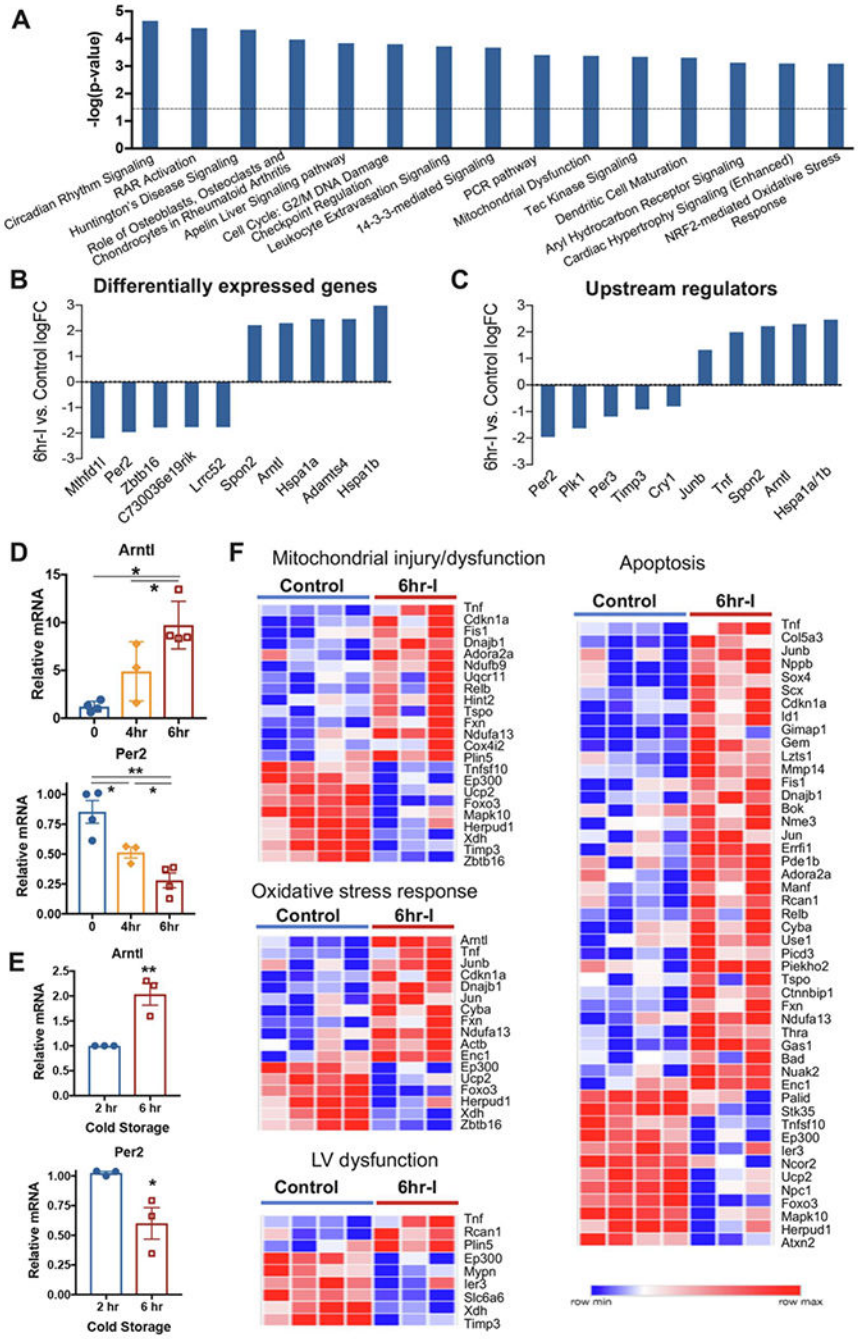

Figure 1. Changes of myocardial transcriptome profile by 6 hr cold storage.

A. Ingenuity Pathway Analysis (IPA) identified top 15 canonical pathways based on p-value. The circadian rhythm pathway was the most disrupted canonical signaling in the hearts with 6 hr cold ischemia (6hr-I, n=3 hearts) compared to no cold storage control (n = 4 hearts). **B.** The most differentially expressed genes (5 down-regulated and 5 up-regulated) by 6hr-I identified using IPA. **C.** Top 5 inhibited and 5 activated upstream regulators in mouse hearts following 6hr-I identified using IPA. **D.** Myocardial Arntl and Per2 transcript levels in isolated mouse hearts (RT-qPCR using TaqMan gene expression assay) in groups of no cold

storage control (n = 4 hearts), 4hr-I (n = 3 hearts) and 6hr-I (n = 4 hearts). **E.** Myocardial mRNA levels of Arntl and Per2 in human hearts (n=3 hearts) following *ex vivo* cold storage using TaqMan gene expression assay. Mean +/− SEM, *p<0.05, **p<0.01 in D and E using student t-test. **F.** Differentially expressed genes involved in mitochondrial injury/dysfunction, oxidative stress response, left ventricular (LV) dysfunction, and apoptosis in mouse hearts exposed to 6hr-I (n = 3 hearts) vs. control (n = 4 hearts) identified using IPA. Heatmap was constructed using counts per million reads of differentially expressed genes by Morpheus (https://software.broadinstitute.org/morpheus). Differentially expressed genes (fold change ≥ 1.5, FDR < 0.1) were used for analyses.

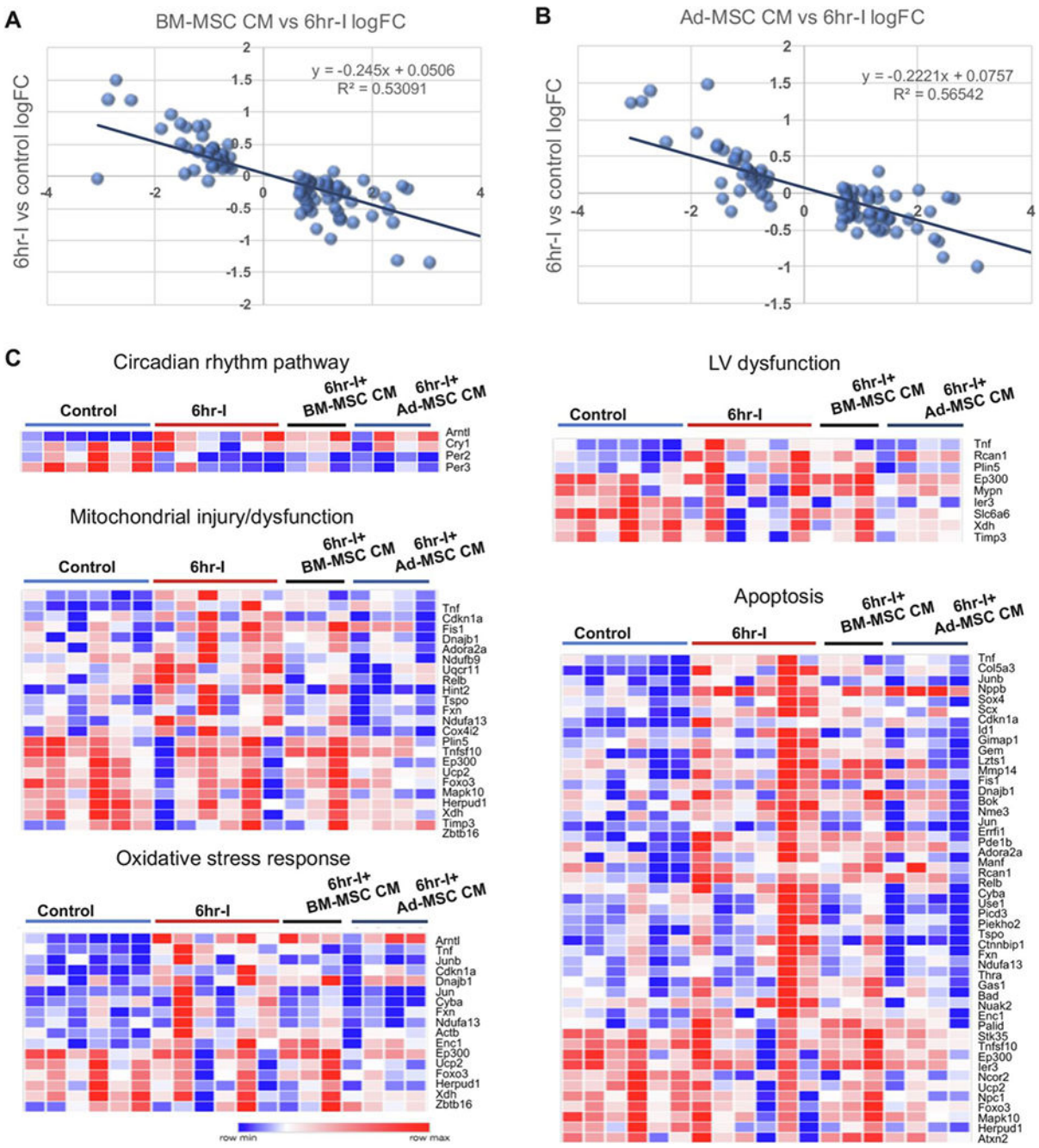

Figure 2. MSC secretome restored myocardial transcriptome profiling towards non-ischemic control levels.

A. BM-MSC CM (conditioned medium) (n = 3 hearts) and **B.** Ad-MSC CM (n = 4 hearts) preserved 6hr-I-induced alterations of myocardial transcriptome profile. Differentially expressed genes (fold change ≥ 1.5, FDR < 0.1) in 6hr-I mouse hearts vs. control were used for analyses. The logFC (fold change) of expression in untreated ischemic hearts (6hr-I) vs. non-ischemic hearts (control) was plotted on the Y-axis, and the logFC of expression in BM-MSC or Ad-MSC CM-treated ischemic hearts vs. 6hr-I hearts on the X-axis. The

differentially expressed genes demonstrated restoration towards normal by MSC CM. **C.** MSC CM preserved 6hr-I induced differential expression of genes involved in circadian pathways, mitochondrial injury/dysfunction, oxidative stress response, left ventricular (LV) dysfunction, and apoptosis. Heatmap was constructed from two batches' data (n = 6 hearts in control [4 from batch 1 and 2 from batch 2 due to one outlier removed in batch 2; 6 hearts in 6hr-I [3 from each batch]; n = 3 hearts in BM-MSC CM and n = 4 hearts in Ad-MSC CM [all from batch 2]) and using Morpheus online software (https://software.broadinstitute.org/morpheus). To avoid the effect of batches, counts per million reads (CPM) of differentially expressed genes as shown in Figure 1 were normalized to their CPM of GAPDH, respectively.

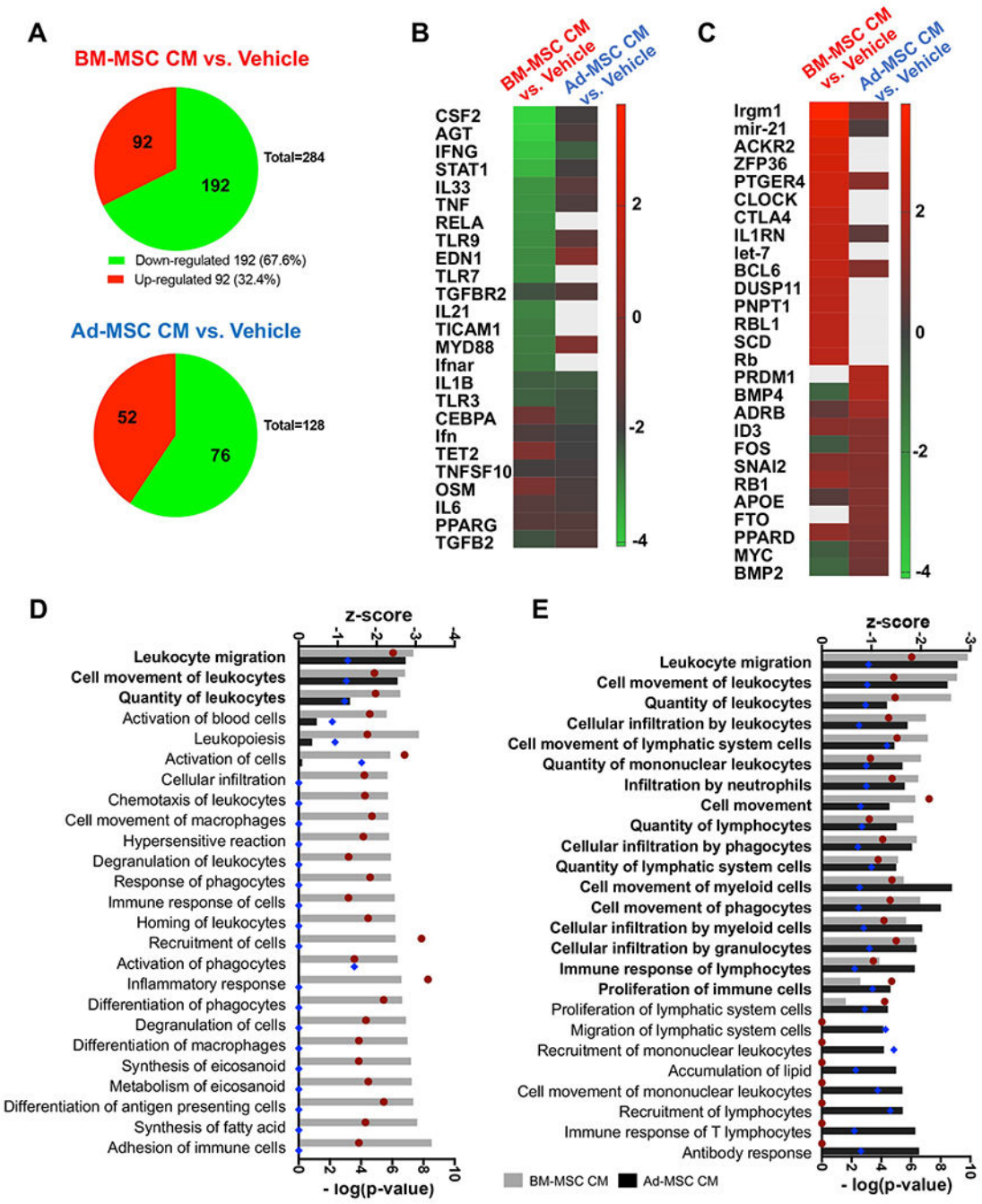

Figure 3. Comparison of BM-MSC CM with Ad-MSC CM on altering myocardial transcriptome profile following 6hr-I.

A. Pie charts indicating the number of differentially expressed genes (FC >= 1.5, p<0.05) that were down-regulated (green) and up-regulated (red) by BM-MSC CM (n = 3 hearts) or Ad-MSC CM (n = 4 hearts) in 6hr-I hearts (vehicle). **B.** Upstream regulators inhibited by BM-MSC CM (top 15 based on z-score) and Ad-MSC CM (top 15) in 6hr-I mouse hearts using the IPA-derived analysis. A total of 25 is shown due to 5 overlapped. **C.** Upstream regulators activated by BM-MSC CM (top 15) and Ad-MSC CM (top 15) in 6hr-I mouse

hearts, shown as 27 (3 overlapped). White square indicates no value obtained in B and C.

D. E. The IPA-based analysis predicted top 25 Diseases and Functions associated with 6hr-I based on z-score of BM-MSC CM (**D**) and Ad-MSC CM (**E**). Bar indicates z-score (gray: BM-MSC CM; black: Ad-MSC CM) and dot is p-value (red: BM-MSC CM; blue: Ad-MSC CM).

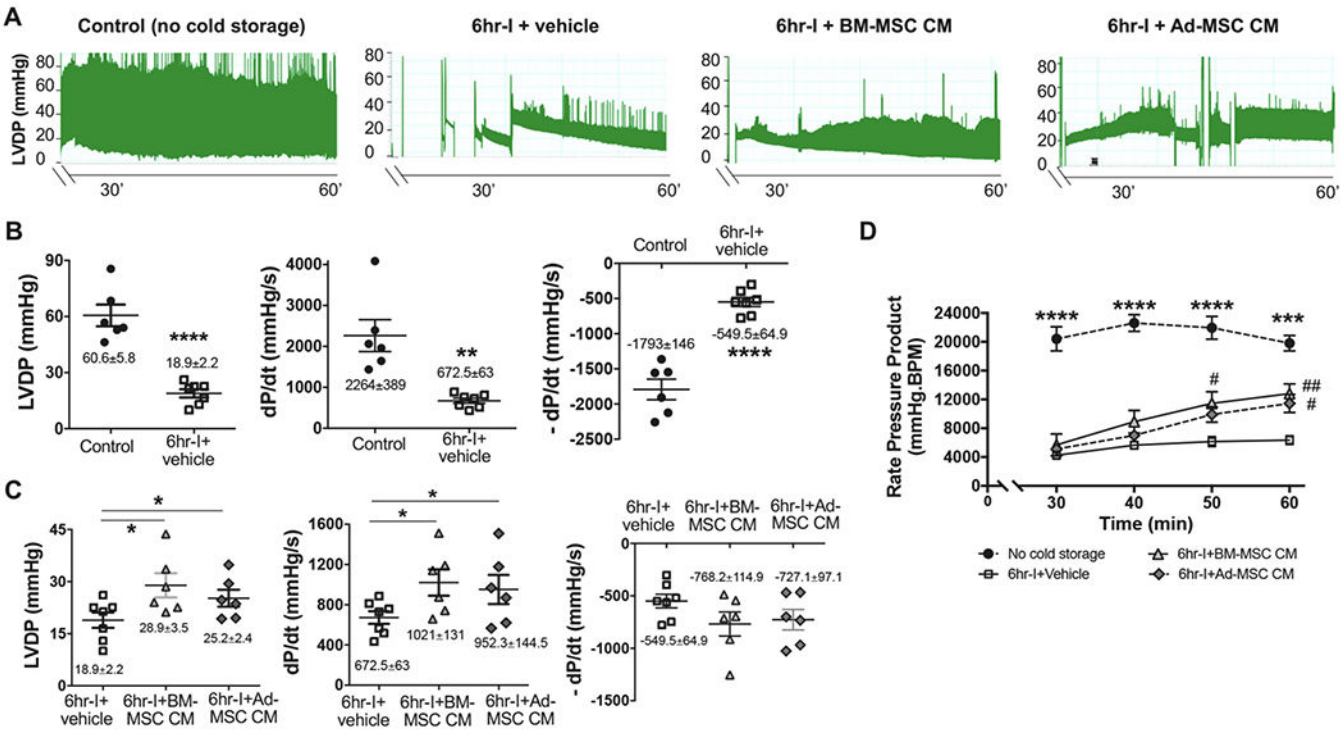

Figure 4. MSC secretome preserved left ventricular (LV) function of donor hearts following 6hr cold storage (6hr-I).

A. LV developed pressure (LVDP) recording trace during reperfusion. **B.** 6hr-I significantly impaired heart function of LVDP, dP/dt and - dP/dt at the end of reperfusion. Mean+/−SEM, **p<0.01, ****p<0.0001 using student t-test. **C.** Effects of BM-MSC CM and Ad-MSC CM on myocardial recovery of LVDP, dP/dt and – dP/dt at the end of reperfusion. Mean+/−SEM, *p<0.05using student t-test. **D.** Changes of rate pressure product (RPP = LVDP x heart rate) among groups of no cold storage (control) and 6hr-I hearts +/− MSC CM. Mean+/−SEM, ***p<0.001, ****p<0.0001 control vs. all other groups, #p<0.05, ##p<0.01 vs. Vehicle. Two-way ANOVA with Tukey's multiple comparison test was utilized. CM: conditioned medium. B – D: n = 6 mouse hearts per group in control (no cold storage), 6hr-I + BM-MSC CM, and 6hr-I + Ad-MSC CM, n = 7 hearts in 6hr-I + vehicle.

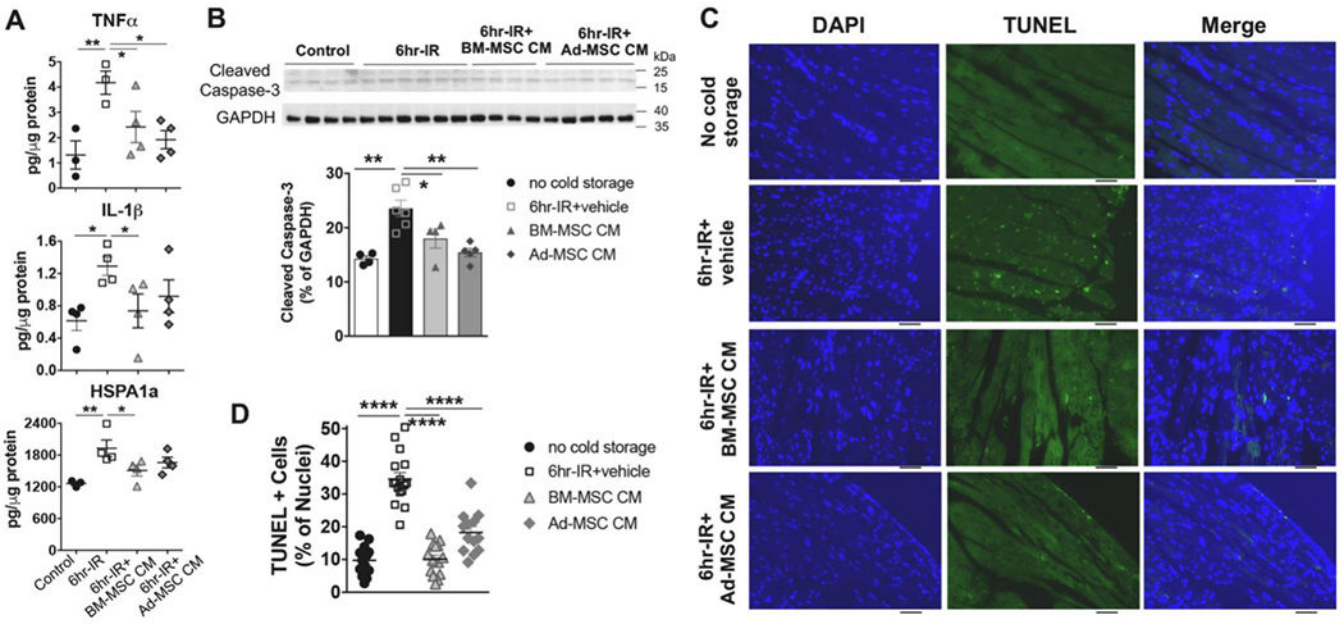

Figure 5. MSC secretome decreased myocardial production of inflammatory cytokines and reduced apoptosis in donor hearts following 6hr cold storage and subsequent reperfusion (6hr-IR).

A. Myocardial protein levels of TNF-α, IL-β, and HSPA1a were determined by ELISA (each dot represented for one individual heart sample). Mean+/−SEM, *p<0.05, **p<0.01 using student t-test. **B.** Pro-apoptotic signal of cleaved Caspase 3 was detected by Western blotting. Bar graph shows immunoblotting band intensity normalized to GAPDH (n = 4 hearts/group in control and 6hr-IR+BM-MSC CM, n = 6 hearts in 6hr-IR + vehicle, and n = 5 hearts in 6hr-IR+Ad-MSC CM). Mean+/−SEM, *p<0.05, **p<0.01 using student t-test. **C.** TUNEL staining of apoptosis in mouse hearts without or with 6hr-IR +/− MSC CM. Shown are representative images of TUNEL assay. The nuclei were stained with DAPI (blue) and apoptotic cells as green (TUNEL +). Scale bar = 50 μm. **D.** Quantitative analysis of TUNEL + cells represented as % of nuclei (n = 3 hearts per group, each dot for one random field, and at least 4 fields per heart). All represented as Mean+/−SEM and used student t-test, ****p<0.0001.

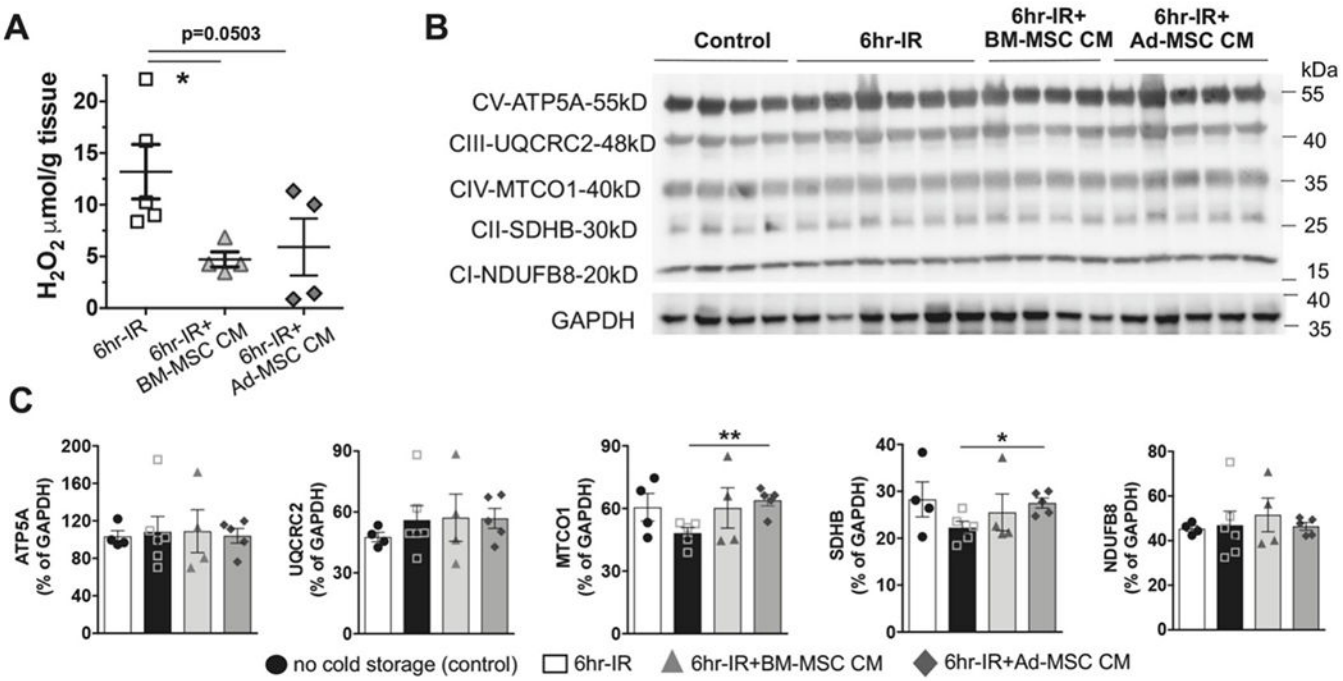

Figure 6. Myocardial levels of H_2O_2 and OXPHOS in mouse hearts following 6hr cold storage and subsequent reperfusion (6hr-IR).

A. Myocardial H_2O_2 level was assessed in mouse hearts subjected to 6hr-IR (each dot for one individual heart sample). Mean+/−SEM, *p<0.05 using student t-test. **B.** Myocardial expression of OXPHOS was detected by Western blotting. **C.** Bar graphs indicate quantification of immunoblotting band intensity of complex I-NDUFB8, complex II-SDHB, complex IV-MTCO1, complex III-UQCRC2, and complex V-ATP5A, represented as % of GAPDH. Mean+/−SEM, *p<0.05 using student t-test, n = 4 hearts/group in control and 6hr-IR + BM-MSC CM, n = 6 hearts in 6hr-IR + vehicle, and n = 5 hearts in 6hr-IR + Ad-MSC CM.

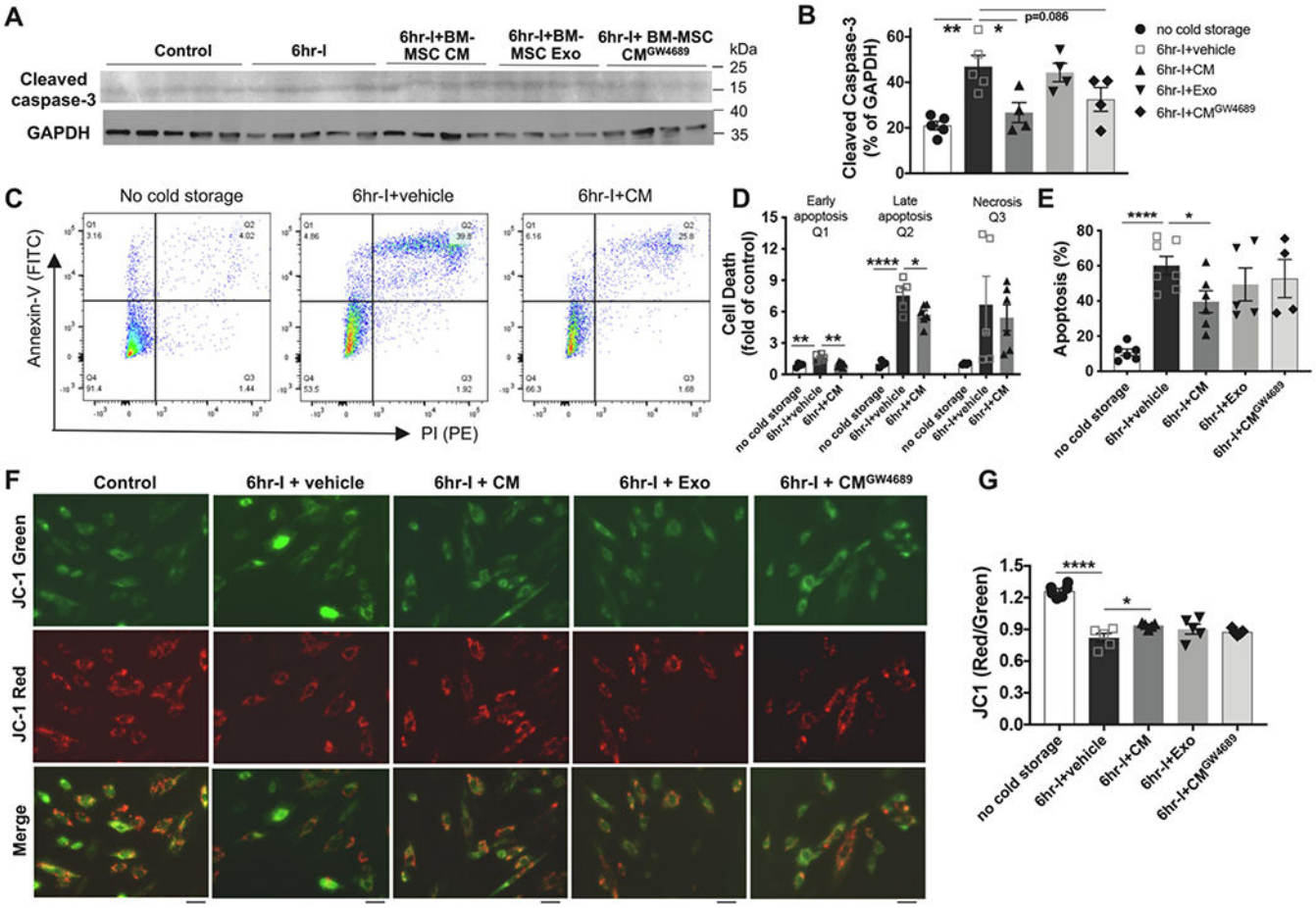

Figure 7. Effects of MSC secretome components on cell apoptosis and mitochondrial membrane potential (MtMP) following cold ischemic storage.

A. Pro-apoptotic signal of cleaved Caspase 3 expression in mouse hearts subjected to 6hr cold storage without reperfusion. Media vehicle, BM-MSC CM, BM-MSC exosomes (Exo), or exosome-depleted MSC CM (CM^{GW4689}) was supplemented to UW solution during cold storage. **B.** Bar graph showed immunoblotting band intensity normalized to GAPDH. Each dot for one individual heart sample (in other words, n = 5 hearts/group in control and 6hr-I, n = 4 hearts/group in 6hr-I+BM-MSC CM, 6hr-I+BM MSC-Exo and 6hr-I+BM MSC-CM^{GW4689}). Mean+/−SEM, *p<0.05, **p<0.01 using student t-test. **C.** Apoptosis in H9c2 cells in response to 6hr cold storage was determined by flow cytometry. Representative images indicated percentages of the population in different regions (Q1: early apoptotic cells [Annexin V+/PI−], Q2: late apoptotic cells [Annexin V+/PI+], Q3: necrotic cells [Annexin V−/PI+], and Q4: viable cells [Annexin V−/PI−]). **D.** BM MSC-CM reduced both early and late apoptosis in H9c2 cells following 6hr cold storage. Each dot for one cell sample (at least two cell samples/condition/trial with a total of three trials). Mean+/−SEM, *p<0.05, **p<0.01, ****p<0.0001 using student t-test. **E.** Apoptosis (Q1+Q2) of H9c2 cells in all groups. Each dot for one cell sample (at least two cell samples/condition/trial with a total of three trials). Mean+/−SEM, *p<0.05, ****p<0.0001 using student t-test. **F.** Representative images of MtMP (with brightness and contrast enhanced) using JC-1 in H9c2 cells after 6hr cold storage. **G.** Red (excitation: 535nm; emission: 585nm) and green (excitation: 485nm;

emission: 535nm) fluorescence intensity in each well was obtained using a microplate reader. The red to green fluorescence intensity ratio was analyzed to indicate MtMP. The graph shown is for a single experiment representative of three trials. Each dot represented for one well (at least 4 wells/condition/trial). Mean+/−SEM,*$p<0.05$, ****$p<0.0001$ using student t-test.

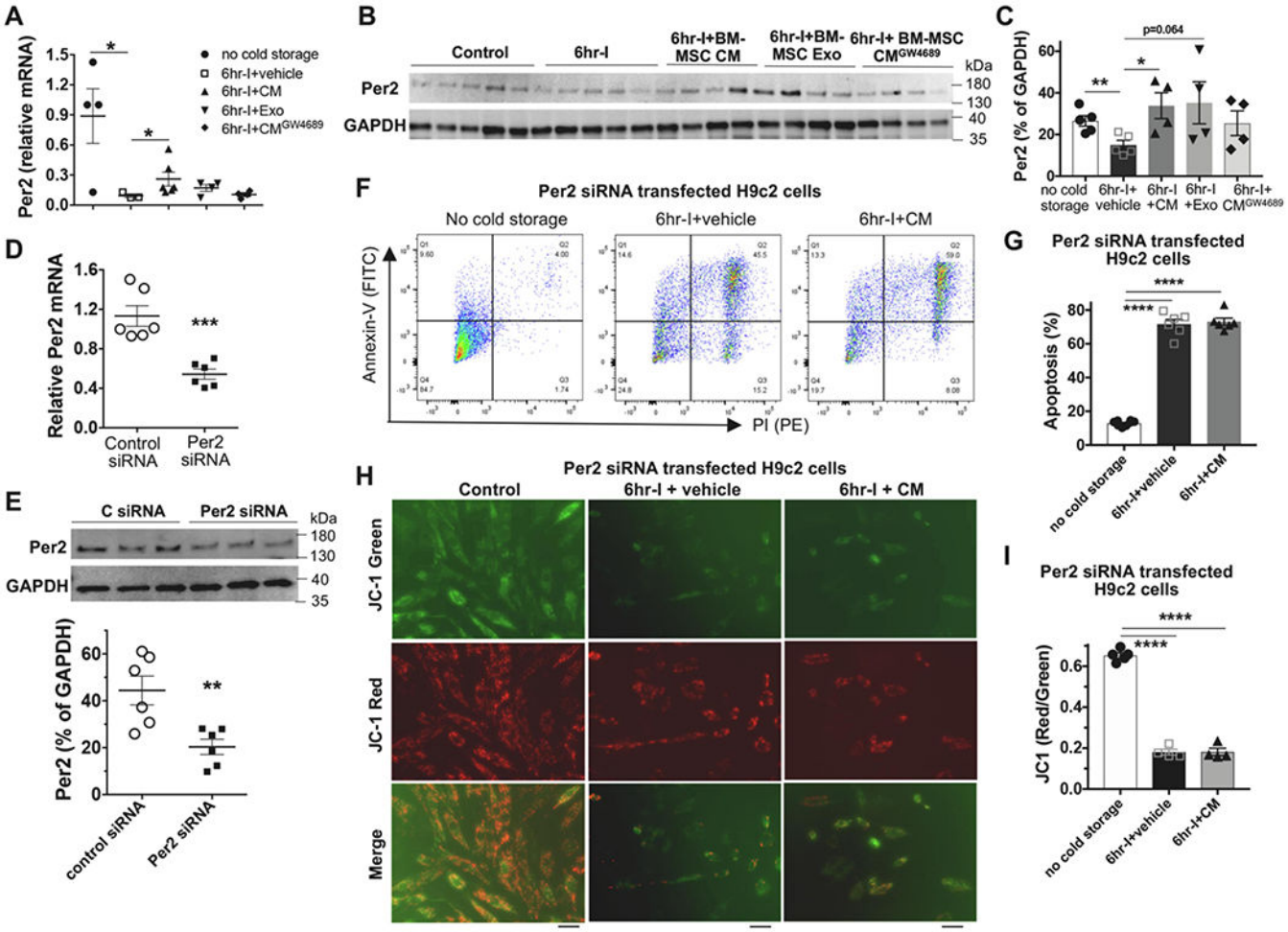

Figure 8. Role of myocardial Per2 in MSC CM-mediated heart preservation following cold storage.

A. Cardiac Per2 transcript levels among groups of no cold storage (control), 6hr-I, 6hr-I+MSC-CM, 6hr-I+MSC-Exo, and 6hr-I+MSC-CM^{GW4869} using TaqMan gene expression assay. Each dot for one individual heart sample (in other words, n = 4 hearts in control, n = 3 hearts in 6hr-I, n = 6 hearts in 6hr-I+BM-MSC CM, and n = 4 hearts/group in 6hr-I+BM MSC-Exo and 6hr-I+BM MSC-CM^{GW4689}). Mean+/−SEM, *p<0.05 using student t-test. **B.** Immunoblots of myocardial Per2 protein. **C.** Densitometry data of Per2 immunoblotting band intensity normalized to GAPDH. Each dot for one individual heart sample (in other words, n = 5 hearts/group in control and 6hr-I, n = 4 hearts/group in 6hr-I+BM-MSC CM, 6hr-I+BM MSC-Exo and 6hr-I+BM MSC-CM^{GW4689}). Mean+/−SEM, *p<0.05, **p<0.01 using student t-test. **D.**mRNA and **E.** protein levels of Per2 in H9c2 cells transfected with Per2 siRNA compared to control siRNA group using TaqMan gene expression assay and Western Blot assay. Each dot represented for one cell sample from one-well cells transfected with control siRNA or Per2 siRNA (three wells/condition/trial with a total of two trials). Mean+/−SEM, **p<0.01, ***p<0.001 using student t-test. **F.** Representative images of apoptosis in H9c2 cells transfected with Per2 siRNA after 6hr cold storage. **G.** Knockdown of Per2 abolished MSC CM-reduced apoptosis in H9c2 cells in response to 6hr cold

ischemia. Each dot for one cell sample (at least two cell samples/condition/trial with a total of three trials). Mean+/−SEM, ****p<0.0001 using student t-test. **H.** Representative images of MtMP using JC-1 in Per2 siRNA-transfected H9c2 cells after 6hr cold storage. Scale bar = 50 μm. **I.** Red (excitation: 535nm; emission: 585nm) and green (excitation: 485nm; emission: 535nm) fluorescence intensity in each well was obtained using a microplate reader. The red to green fluorescence intensity ratio was analyzed to indicate MtMP in H9c2 cells transfected with Per2 siRNA. The graph shown is for a single experiment representative of three trials. Each dot for one well (at least 4 wells/condition/trial). Mean+/− SEM, ****p<0.0001 using student t-test.

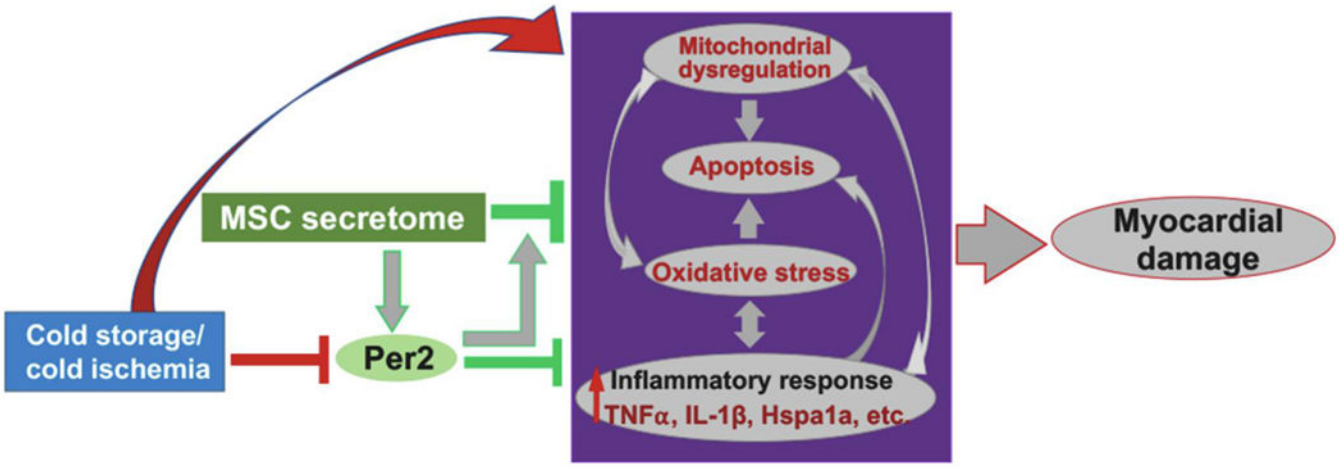

Figure 9. Proposed model of cold storage/ischemia-induced myocardial damage and MSC secretome-mediated protection in donor hearts.

Six-hour cold storage/ischemia triggers myocardial maladaptive response (red arrow), including increased inflammatory response, oxidative stress, and apoptosis, as well as dysregulated mitochondrial performance. All these lead to myocardial damage in donor hearts. Prolonged cold storage also induces disrupted circadian signaling with reduction of myocardial Per2, which further aggravates detrimental effects of cold ischemia on myocardium. MSC secretome prevents these maladaptive responses and increases Per2 expression, thus protecting donor hearts against cold ischemia.